

Cardiac reporter gene imaging using the human sodium/iodide symporter gene

Masao Miyagawa^{a,1}, Moritz Beyer^{a,1}, Bettina Wagner^a, Martina Anton^b, Christine Spitzweg^c,
Bernd Gansbacher^b, Markus Schwaiger^a, Frank M. Bengel^{a,*}

^aNuklearmedizinische Klinik und Poliklinik, Technische Universität München, Klinikum rechts der Isar, Ismaninger Str. 22, 81675 München, Germany

^bInstitut für Experimentelle Onkologie und Therapieforchung, Technische Universität München, Munich, Germany

^cMedizinische Klinik II, Ludwig Maximilians Universität München, Munich, Germany

Received 5 July 2004; received in revised form 19 September 2004; accepted 1 October 2004

Available online 27 October 2004

Time for primary review 17 days

Abstract

Objective: Imaging of reporter gene expression holds promise for noninvasive monitoring of cardiovascular molecular therapy. We investigated the feasibility of myocardial gene expression imaging in living rats using the human sodium/iodide symporter gene (hNIS) and widely available scintigraphic techniques.

Methods: We injected adenovirus expressing hNIS under control of cytomegalovirus promoter (Ad_{hNIS}) directly into left ventricular myocardium of Wistar rats. For detection of reporter gene expression, dynamic gamma-camera imaging was performed following intravenous injection of ¹²³Iodide or ^{99m}Technetium.

Results: For both radiotracers, focal cardiac accumulation was identified as early as 10 min, and remained detectable until 2 hrs after injection, while it was not present in animals injected with LacZ control virus. Intensity of tracer accumulation gradually decreased when decreasing titers of Ad_{hNIS} were applied. Treatment with sodium perchlorate (a blocker of hNIS) abolished cardiac tracer uptake after Ad_{hNIS}-infection. Serial imaging after cardiac gene transfer demonstrated a peak of tracer signal between days 1 and 3, and a subsequent decrease until day 12. Postmortem analysis of hearts yielded significant correlation between in vivo radiotracer accumulation and ex vivo gamma-counting. Autoradiography demonstrated specific regional radioactivity in Ad_{hNIS}-infected myocardial areas.

Conclusions: hNIS offers a practical and reliable approach for myocardial gene expression imaging. Using suitable vectors, hNIS may be coexpressed with therapeutic genes or stably expressed in stem cells for future monitoring of cardiovascular molecular therapy.

© 2004 European Society of Cardiology. Published by Elsevier B.V. All rights reserved.

Keywords: Radionuclides; Cardiac imaging; Gene expression; Gene therapy; Reporter genes; Sodium/iodide transporter

1. Introduction

Gene and cell therapy hold great promise for treatment of heart disease [1,2]. Translational efforts from experimental to clinical settings are increasing and the need for imaging tools to monitor molecular therapy is increasingly emphasized. Imaging the expression of reporter genes by use of radio-

labeled reporter probes has great potential in this regard. Suitable reporter genes can be coexpressed together with therapeutic genes or within transplanted cells, and radionuclide imaging will allow for assessment of location, magnitude, and persistence of transgene expression in the heart and the whole body [3–6]. This methodology is expected to be helpful for further development of molecular therapy by helping (a) to identify the optimal method for gene or cell delivery in a given situation, (b) to determine therapeutic efficacy individually, and (c) to visualize time course of gene expression and/or fate of transplanted cells in target and remote areas.

* Corresponding author. Tel.: +49 89 4140 2971; fax: +49 89 4140 4950.

E-mail address: frank.bengel@lrz.tum.de (F.M. Bengel).

¹ Both authors (MM and MB) contributed equally to this work.

Recently, positron emission tomography (PET)-based myocardial gene expression imaging has been reported in living animals using herpes simplex virus type 1 thymidine kinase gene (HSV1-tk) as reporter gene and positron-labelled substrates as reporter probe [3–6]. PET is well suited for in vivo imaging of biological processes because of its high sensitivity for probe detection and quantitative tomographic information. However, because of the requirement for PET scanners and on-site radiochemical synthesis by an experienced radiochemist, widespread use of this method is limited. As such, a method that uses more easily available instruments and simple radioisotopes would benefit the broad application of cardiac gene expression imaging.

Sodium/iodide symporter (NIS) is an intrinsic transmembrane glycoprotein, which mediates active transport of iodide and sodium across the cytoplasmic membrane. In the thyroid gland, where it is naturally expressed, it facilitates accumulation of iodide by follicular cells to concentrations 20- to 40-fold over plasma levels, which is essential for production of thyroid hormones [7]. The potential for iodine concentration of thyroid cells allows for diagnostic scintigraphy with the radioisotopes ^{123}I , ^{131}I , and $^{99\text{m}}\text{Tc}$ -pertechnetate ($^{99\text{m}}\text{Tc}$), whose uptake is also mediated by NIS. Both the rat and human NIS (hNIS) genes were cloned and have been shown to be functional in vitro when expressed in nonthyroidal cells from different species [8,9]. hNIS would be an attractive alternative to the previously used HSV1-tk for cardiac reporter gene imaging. It is normally not expressed in cardiac cells and can be imaged easily with widely available radionuclides and conventional gamma-camera systems. Additionally, it is nonimmunogenic in humans, which is in contrast to previously used HSV1-tk and facilitates its potential future use in a clinical setting. The purpose of this study was to investigate the use of hNIS as a new reporter gene for imaging of cardiac transgene expression in living animals.

2. Methods

2.1. Adenoviral vectors

Replication-defective type 5 adenoviral vector expressing human NIS (Ad_{hNIS}) under transcriptional control of human cytomegalovirus early gene promoter were developed in collaboration with the Gene Transfer Vector Core Facility of the University of Iowa (Iowa City, IA, USA) [10]. A vector that carried the LacZ gene (Ad_{LacZ}) was used as negative control [11]. Double cesium chloride-purified vectors were used throughout the study and titres were determined by plaque assay on 293 cells [12]. Adenoviral vector preparation was tested for replication competent adenovirus by PCR (forward primer 5'–AGGCCGCCAGTCTTTT–3' reverse primer 5'–GCCATGCAAGTTAAACATTATC–3') and was found to be negative in 1×10^9 plaque-forming units (pfu).

2.2. Rat experimental protocol

Experimental protocols were approved by the regional governmental commission of animal protection (Regierung von Oberbayern) and the investigation conforms with the Guide for the Care and Use of Laboratory Animals published by the US National Institutes of Health. Under anesthesia with intramuscular injection of midazolam (0.1 mg/kg), fentanyl (1 $\mu\text{g}/\text{kg}$), and medetomidine (10 $\mu\text{g}/\text{kg}$), a total of 39 male Wistar rats (220–250 g) underwent injection of adenoviral vectors. They were injected percutaneously with use of a 26-gauge, 1-in. needle into inferior left ventricular myocardium from epigastric angle under echocardiographic guidance [13]. For echocardiography, a 10-MHz probe was fixed on a tripod and intramyocardial injection was continuously monitored by ultrasound during the vector administration procedure. The virus suspension of 200 μL was slowly injected to each rat myocardium. A localized high-echo area was observed at injection sites directly after viral injection, suggesting successful injection and presence of a fluid deposition. When echocardiography was repeated at 30 min after injection, the intramyocardial signal had disappeared, suggesting absence of a persisting fluid pocket. No other structural abnormalities were observed at echocardiography. This is in line with previous reports and suggests a lack of major histologic alterations due to the injection [13].

2.3. Detection sensitivity for imaging gene expression

Ad_{hNIS} with viral titers of 2.5×10^9 , 5×10^8 , 1×10^8 , and 2×10^7 plaque-forming units (pfu, $n=6$ for each titer) or control virus (Ad_{LacZ} with 2.5×10^9 pfu, $n=6$) was directly injected into the rat myocardium to determine the lowest viral titer needed for imaging gene expression. Dynamic in vivo imaging with a gamma-camera followed the next day (30 hrs after viral injection) for 120 min after intravenous radiotracer injection (three animals with ^{123}I and three animals with $^{99\text{m}}\text{Tc}$ in each group).

2.4. Perchlorate inhibition study

For perchlorate inhibition studies, sodium perchlorate was given orally during 24 hrs before the imaging of 6 rats with Ad_{hNIS} at a viral titer of 2.5×10^9 pfu. Imaging followed the next day (30 hrs after viral injection) for 120 min after intravenous radiotracer injection (three animals with ^{123}I and three animals with $^{99\text{m}}\text{Tc}$). Subsequently, Northern blot analysis was performed for ex vivo validation.

2.5. Time course study

The time course of myocardial $^{99\text{m}}\text{Tc}$ accumulation was examined in three rats with Ad_{hNIS} (2.5×10^9 pfu) by

serial imaging at 4, 30, 72, 120, 192, and 288 hrs after vector application. In this setting, 10-min planar scintigraphy was obtained 1 hr after intravenous ^{99m}Tc injection.

2.6. Dynamic gamma-camera imaging

For imaging, rats were anesthetized and placed in a prone position on one detector head of a dual-headed gamma-camera (Skylight, ADAC/Philips, Hamburg, Germany) equipped with a low-energy, high-resolution collimator. The second detector head was then positioned as close as possible (approximately 5 mm) to the back of the animals (ventral-dorsal view, the intrinsic spatial resolution was 3.2 mm at full-width at half-maximum according to the manufacturer). Whole body imaging was started immediately after tail-vein injection of 20 MBq ^{123}I or 40 MBq ^{99m}Tc . A total of 12 serial scintigraphic images with ventral (anterior) and dorsal (posterior) views of 10 min each were acquired in 512×512 matrices with a zoom factor of 1.0 (pixel size, 1.24 mm) and a photopeak window set at 15% around 159 keV for ^{123}I or 140 keV for ^{99m}Tc .

To quantify cardiac radiotracer accumulation, circular, 200 pixel-sized regions of interest (ROIs) were manually drawn around the heart on both anterior and posterior images. This cardiac ROI was approximately 15–30% greater than the actual size of a normal rat heart due to magnification effects in a projection image and due to the influence of Compton scattering with gamma rays from the heart. The injected dose (ID) was defined as the total number of counts within another set of ROIs encompassing the total body (approximately 7500–9000 pixels). Then, cardiac radiotracer accumulation was expressed as percent of injected dose (%ID) using the following equation based on calculation of geometric means:

Cardiac accumulation (%ID)

$$= \sqrt{\left(\frac{C_{ant}}{B_{ant}}\right) \left(\frac{C_{post}}{B_{post}}\right)} \times 100$$

Cant: total counts in the anterior cardiac ROI; *Cpost*: total counts in the posterior cardiac ROI; *Bant*: total counts in the anterior whole body ROI; *Bpost*: total counts in the posterior whole body ROI.

2.7. Ex vivo analysis

2.7.1. Biodistribution, autoradiography, and β -galactosidase staining

After gamma-camera imaging, all animals were euthanized. Hearts were immediately taken, rinsed with saline solution, and weighed. Radioactivity in each organ was measured with a gamma-counter (Cobra Quantum, Packard Instruments Company, Meriden, USA). Results were expressed as the percentage of the injected dose per gram (%ID/g) tissue.

After gamma-counting, hearts were rapidly frozen. Short axis slices with a thickness of 40 μm were prepared (HM5000M microtome, Microm, Walldorf, Germany) and digital autoradiography (Phosphorimager 445 SI, Molecular Dynamics, Sunnyvale, CA) was performed for all slices from an animal on the same imaging plate. Ratios of maximal counts in virus injection areas relative to remote area were calculated.

LacZ gene expression was assessed by β -galactosidase staining in rats injected with Ad_{LacZ} to identify virus injection site and confirm successful intramyocardial injection of the control vector [14].

2.7.2. Northern blot analysis

Frozen hearts were homogenized using an Ultra-Turrax T25 (IKA Labor Technik, Staufen, Germany). Total RNA was extracted from hearts using RNeasy Mini Kit (Qiagen, Hilden, Germany) according to the manufacturer's instructions for RNA extraction from the heart. RNA was separated on denaturing agarose gels, transferred to GeneScreen hybridization transfer membranes (Perkin Elmer Life Sciences, Zaventem, Belgium), and UV cross-linked. A hNIS internal *PstI* fragment was labeled with α ^{32}P -dCTP (ICN Biomedicals, Eschwege, Germany) using Prime-It II Random Primer Labeling Kit (Stratagene, Amsterdam, The Netherlands). Hybridization was done under standard conditions [15]. Membranes were exposed to FLA-2000 PhosphoImager (raytest, Straubenhardt, Germany). After stripping, membranes were first rehybridized with a LacZ internal *PvuI* fragment and after additional stripping rehybridized with 18S-coding DNA fragment as loading control.

2.8. Statistical analysis

Results are described as mean \pm standard error of the mean (S.E.M.). One-way ANOVA with the least-square differences post hoc test was used for comparison of the control group with study groups of four different viral titers. Student's *t*-test was employed to compare cardiac uptake in animals with and without perchlorate blockade. Receiver operating characteristics (ROC) curve analysis was used to identify the optimal quantitative value of cardiac tracer accumulation, which reflects visual detectability [4]. Spearman's rank correlation was performed to analyze the relationship between %ID calculated from scintigraphy and from gamma-counting. Probability values <0.05 were considered statistically significant.

3. Results

3.1. Characterization of sequential in vivo images

Representative planar gamma-camera images of radiotracer distribution after injection of adenovirus at the highest

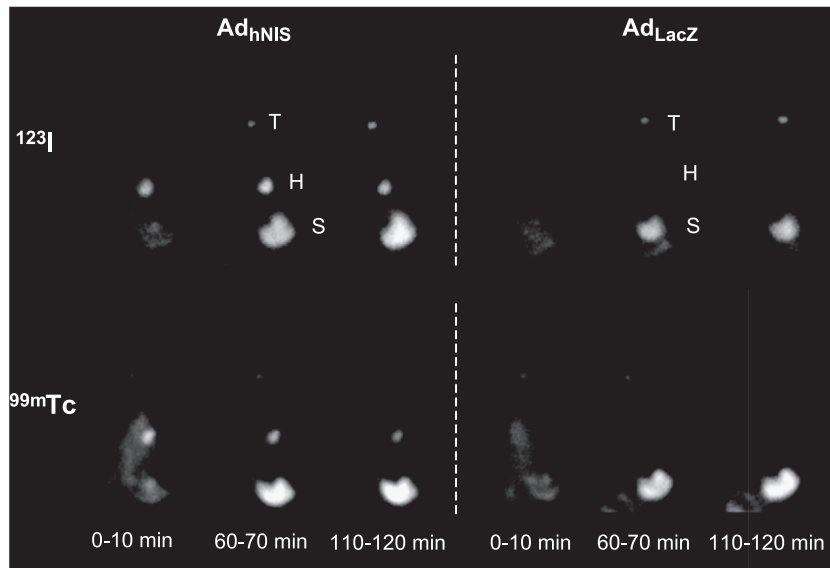


Fig. 1. Whole-body images of representative rats at 0–10, 60–70, and 110–120 min after intravenous injection of ^{123}I (top) and $^{99\text{m}}\text{Tc}$ (bottom), which were obtained 30 h after intramyocardial injection of Ad_{hNIS} (left) or Ad_{LacZ} (right) with virus titers of 2.5×10^9 pfu. Additionally, physiological gastric and thyroid uptake of ^{123}I or $^{99\text{m}}\text{Tc}$ is seen on each image. Grey scale is normalized to individual peak activity of each image. T: thyroid, H: heart, S: stomach.

viral titer are depicted in Fig. 1. Qualitatively, focal accumulation was visualized in the cardiac region of Ad_{hNIS} -injected rats during the entire 2-hr imaging period using either ^{123}I or $^{99\text{m}}\text{Tc}$ as radiotracer. In control animals, only blood-pool radioactivity was present in the cardiac region at early after injection, but no persisting focal accumulation was detected.

The magnitude of quantitatively measured cardiac accumulation of both tracers in animals receiving the highest vector dose ($n=3$ per group) is shown in Fig. 2. Cardiac uptake showed higher values in Ad_{hNIS} -injected rats than in controls at all time points until the end of imaging. Washout from the heart was observed for both tracers. Efflux rates from the heart over the imaging period of 2 hrs

were $46.7 \pm 2.4\%$ for $^{99\text{m}}\text{Tc}$ and $26.5 \pm 6.5\%$ for ^{123}I in Ad_{hNIS} -injected rats, while they were $60.5 \pm 0.4\%$ for $^{99\text{m}}\text{Tc}$ and $25.2 \pm 3.3\%$ for ^{123}I in controls. At maximum, cardiac ^{123}I accumulation showed a 2.06 ± 0.18 -fold increase compared to controls at 30–40 min after injection, while cardiac $^{99\text{m}}\text{Tc}$ concentration reached a maximal 1.92 ± 0.12 -fold increase compared to controls at 60–70 min after injection. Uptake at these optimal imaging time points is thus reported in further experiment and is subsequently used for statistical analysis.

Relevant tracer accumulation in organs other than the heart was only found for thyroid and stomach, the two organs with the highest natural expression of NIS. Quantitatively, tracer accumulation for the thyroid in Ad_{hNIS} -

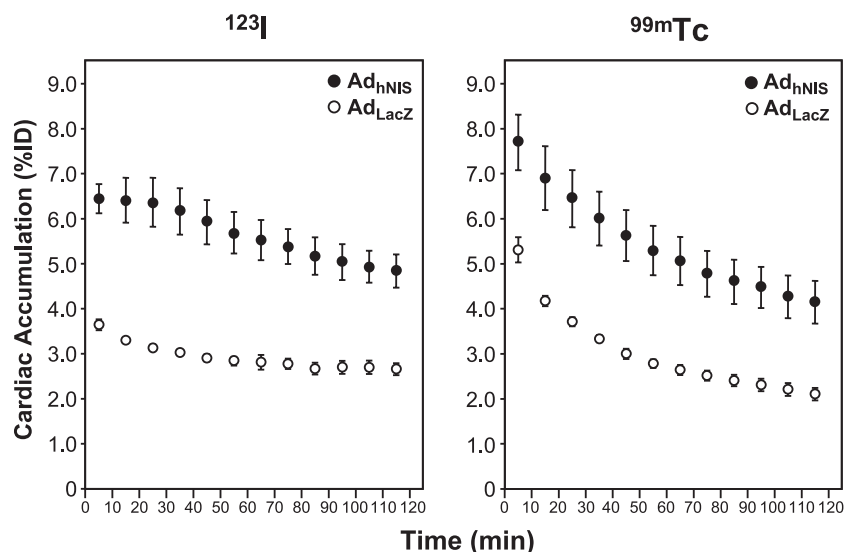


Fig. 2. Time activity curves of cardiac radiotracer accumulation during 2 h after injection of ^{123}I (left) or $^{99\text{m}}\text{Tc}$ (right) in Ad_{hNIS} -injected rats (●) and controls (○; virus titers of 2.5×10^9 pfu) were obtained by ROI analysis ($n=3$ in each group). Values are mean \pm S.E. at each time interval.

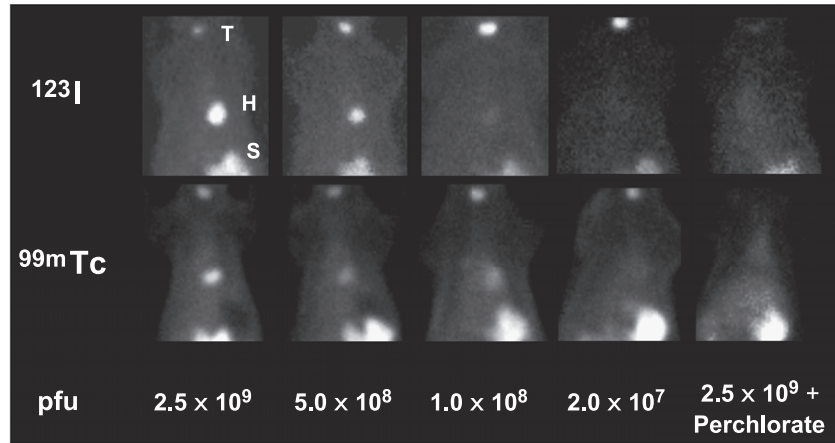


Fig. 3. Thoracic images of representative rat hearts with different viral titers of Ad_{hNIS}. Localized cardiac radiotracer accumulation was visually identifiable with viral titers down to 1×10^8 pfu but not with 2×10^7 pfu. Localized accumulation was not visually identified in sodium perchlorate treated rats with a viral titer of 2.5×10^9 ($n=6$). pfu: plaque-forming units. T: thyroid, H: heart, S: stomach.

injected rats was 1.90 ± 0.10 %ID for ^{123}I and 1.97 ± 0.07 %ID for $^{99\text{m}}\text{Tc}$, respectively. In controls, it was 1.82 ± 0.12 %ID for ^{123}I and 2.29 ± 0.19 %ID for $^{99\text{m}}\text{Tc}$. Tracer accumulation of the stomach in Ad_{hNIS}-injected rats was 13.9 ± 1.08 %ID for ^{123}I and 25.5 ± 1.95 %ID for $^{99\text{m}}\text{Tc}$. In controls, it was 13.2 ± 2.83 %ID for ^{123}I and 21.4 ± 1.79 %ID for $^{99\text{m}}\text{Tc}$.

3.2. Relationship between reporter probe signal and vector dose

Qualitatively, focal accumulation of ^{123}I in the cardiac region was visually identified in all rats at viral titers of 2.5×10^9 , 5×10^8 pfu and in 2 of 3 rats at a titer of 1×10^8 pfu but not at titer of 2×10^7 pfu. For $^{99\text{m}}\text{Tc}$, focal accumulation in the cardiac region was visually identified in all rats at viral titers of 2.5×10^9 , 5×10^8 , and 1×10^8 pfu but not at a titer of 2×10^7 pfu. Fig. 3 shows examples of representative animals at different viral titers. ROC curve analysis suggests that a %ID value above 2.40 for ^{123}I and 2.50 for $^{99\text{m}}\text{Tc}$, respectively, characterized visually identifiable cardiac tracer accumulation.

Quantitatively, radiotracer accumulation intensity gradually decreased with lowering viral titers. Statistical analysis revealed significantly higher cardiac uptake vs. controls for Ad_{hNIS} titers of 2.5×10^9 and 5×10^8 pfu (Table 1).

3.3. Blockade of radiotracer uptake by sodium perchlorate

Qualitatively, focal radiotracer accumulation of ^{123}I as well as $^{99\text{m}}\text{Tc}$ was not visually identified in sodium perchlorate-treated animals (Fig. 3).

Quantitatively, cardiac tracer uptake was significantly lower for perchlorate-pretreated animals compared to non-pretreated animals at the same Ad_{hNIS} titer ($n=6$ for each group; three animals imaged with ^{123}I , three with $^{99\text{m}}\text{Tc}$; 5.6 ± 0.4 vs. $2.7 \pm 0.1\%$, $P < 0.0001$).

To assure successful gene transfer and gene expression after injection of Ad_{hNIS} and Ad_{LacZ}, total RNA was isolated from rat hearts and analysed by Northern blot. hNIS expression was qualitatively detected in all nontreated ($n=2$) and sodium perchlorate pretreated ($n=2$) Ad_{hNIS}-injected animals, but not in an Ad_{LacZ}-injected control heart ($n=1$).

3.4. Time course of hNIS gene expression

To describe hNIS expression over time, serial imaging was employed until 12 days after intramyocardial injection of Ad_{hNIS} (Fig. 4). Cardiac $^{99\text{m}}\text{Tc}$ accumulation peaked between days 1–3 and gradually decreased up to day 12. Specific cardiac accumulation could be visualized until day 8, but no longer on day 12.

Table 1
Cardiac radiotracer uptake in %ID

Tracer	Control group	Study groups (Ad _{hNIS})			
	(Ad _{LacZ} , 2.5×10^9 pfu)	Group I (2.5×10^9 pfu)	Group II (5×10^8 pfu)	Group III (1×10^8 pfu)	Group IV (2×10^7 pfu)
$^{99\text{m}}\text{Tc}$	$2.62 \pm 0.10^*$	5.03 ± 0.43	3.99 ± 0.15	3.33 ± 0.27	2.39 ± 0.12
^{123}I	$3.00 \pm 0.02^\dagger$	6.16 ± 0.51	3.63 ± 0.10	2.65 ± 0.14	2.40 ± 0.08

Values are mean \pm S.E.; all groups $n=3$. ID=injected dose, Ad=adenovirus, pfu=plaque-forming units of adenoviral vector.

* $p < 0.0001$ vs. group I, $p=0.003$ vs. group II, $p=0.07$ vs. group III.

† $p < 0.0001$ vs. group I, $p=0.10$ vs. group II.

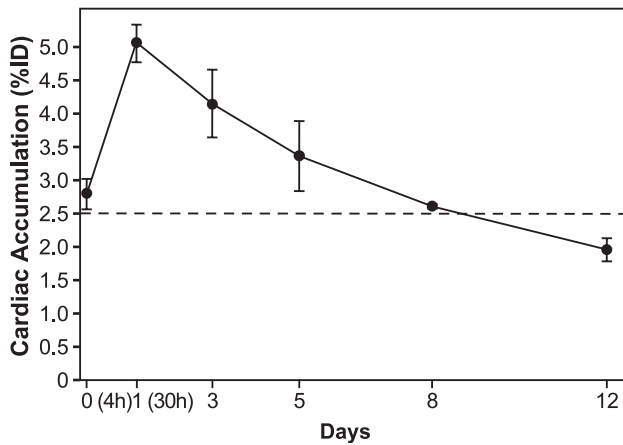


Fig. 4. Time course of %ID for myocardial ^{99m}Tc accumulation calculated from planar images serially scanned in three rats. Broken line indicates cutoff %ID value for visually identifiable ^{99m}Tc accumulation.

3.5. Ex vivo validation

Postmortem analysis yielded significant correlation between global cardiac ^{99m}Tc accumulation measured by in vivo scintigraphy and ex vivo gamma-counting of the whole heart ($R_S=0.88$, $P<0.0001$; $n=18$). Cardiac ^{123}I accumulation by in vivo scintigraphy also correlated significantly with ex vivo gamma-counting ($R_S=0.91$, $P=0.0162$; $n=10$, 5 samples missing due to gamma counter error).

Autoradiography demonstrated specific regional myocardial tracer uptake in areas of Ad_{hNIS} injection, while increased regional radioactivity was absent in control animals after Ad_{LacZ} injection. Successful myocardial delivery of Ad_{LacZ} was specifically identified in all control animals by β -galactosidase staining, while there was no staining in Ad_{hNIS} -injected areas. The count ratio of Ad_{hNIS} -injected areas relative to remote myocardium at the highest viral titer of 2.5×10^9 pfu was 14.19 ± 1.63 for ^{123}I ($n=3$) and 11.03 ± 1.87 for ^{99m}Tc ($n=3$), respectively.

4. Discussion

In summary, this study demonstrates the feasibility of hNIS as reporter gene for noninvasive nuclear imaging of transgene expression in the heart. Scintigraphic images demonstrate specific cardiac accumulation of radioiodine or its analogue pertechnetate after adenoviral myocardial transfer of hNIS, but not after application of control virus. The relationship between imaging signal and vector concentration along with successful blockade of radiotracer uptake by sodium perchlorate, a specific competitive inhibitor of NIS [7–9], give further support to the specificity of the imaging approach for detection of transgene expression. Finally, the usefulness of serial noninvasive imaging was demonstrated by description of the course of transient hNIS expression following adenoviral gene transfer.

Physiologically, NIS is expressed primarily in thyroid tissue, but variable degrees of NIS expression were observed in other tissues including gastric parietal cells, salivary glands, and lactating mammary tissue [16,17]. NIS cotransports one I^- ion with two Na^+ ions into cells [18]. The sodium gradient provides energy for this transfer, as generated by Na^+/K^+ -adenosine triphosphatase [16]. NIS is capable of transporting other monovalent anions, including pertechnetate [18,19]. Perchlorate (ClO_4^-), however, is not transported and acts as a specific inhibitor.

Cloning of the NIS gene has opened new approaches for imaging gene expression by transmitting the ability to accumulate radioiodide to nonthyroid tissue through gene transfer [20–22]. Several investigators reported the successful accumulation of radioiodine [23–26] or ^{99m}Tc [27,28] in several carcinoma cell lines and tumors which were transfected with the NIS gene, although little is known about its usefulness for imaging in cardiac cells. Boland et al. [25] studied adenovirus-mediated transfer of the thyroid sodium/iodide symporter gene into tumors for targeted radiotherapy. Local intratumoral injection with 2×10^9 pfu of Ad_{hNIS} in mice lead to 10.5% of radioactivity taken up in vivo. Spitzweg et al. [10] reported that prostate cancer xenografts in nude mice injected with an adenovirus carrying the NIS gene linked to the cytomegalovirus promoter revealed highly active uptake (20%) of radioiodine. Groot-Wassink et al. [29] could detect the expression of hNIS by PET (3.48 to 7.55 %ID/g of radioiodine) in various sizes of tumor xenografts when the virus was injected intratumorally. Our study applied hNIS as a reporter gene for in vivo imaging of transgene expression in the heart and demonstrated that 6.4% of the total ^{123}I activity was initially taken up by the heart, which was comparable to previous studies of tumors. For tumoricidal therapy, the isotope iodine-131 with a longer half-life of 8 days and beta-emission is used. Scintigraphic imaging in the present study was performed using the short-lived, gamma-emitting isotopes iodine-123 (13-h half-life) and technetium-99 m (6-h half-life). These tracers are well established for clinical thyroid imaging and are known to cause no damage to accumulating tissue.

The NIS protein is not likely to interact with the underlying cell biochemistry in myocardium, since iodide is not metabolised. Although sodium influx may be a concern, no effects have been observed to date. However, there is still the possibility that the membrane potential may differ after Ad_{hNIS} transfection and that depolarisation and repolarisation of transfected myocytes are affected. This issue thus warrants further detailed in vitro and in vivo studies in the future before hNIS can be used as reporter gene on a broader experimental and potentially clinical scale. In our study, all animals were clinically stable throughout the observation period.

The use of reporter genes holds promise for future noninvasive monitoring of cardiac gene therapy by coexpression with a therapeutic gene of choice [30]. Furthermore, reporter genes can be transferred to cells prior to

transplantation for studies of cell trafficking, e.g., in cardiac stem cell therapy [5]. Such great potential emphasizes the need for identifying the most suitable reporter probe and reporter gene combination.

Although we did not measure the exact amount of transgene expressed in myocardium by an independent ex vivo technique, our data nevertheless suggest that hNIS is an attractive reporter gene in the heart, as its unique characteristics compare favorably with previously applied imaging reporter genes such as HSV1-tk and mutant HSV1-sr39tk gene. These reporter genes require the synthesis of complicated substrates and expensive PET equipment. In one previous study, e.g., highly sensitive small animal PET was used to detect a specific total myocardial accumulation of reporter probe in the range of 0.1–0.15 %ID [4]. Despite the different methodology, this strength of cardiac signal appears to be lower when compared to the present study. The fact that conventional planar scintigraphy, which is a less-sensitive method with low resolution, could be used in this study, further supports the usefulness of hNIS as a reporter gene yielding high accumulation of reporter probe. Additionally, hNIS has advantages due to the wide availability of its substrates radioiodine and ^{99m}Tc , which are approved for human use with well-understood metabolism and clearance in the body [18]. There is no problem of labelling stability when using these substrates. In addition, substrates used in the HSV1-tk system can be toxic to cells. Overexpression of a membrane transporter molecule may result in a more rapid decay of transgene expression than in the case of adenoviral overexpression of a cytosolic enzyme, and a recent study using HSV1-tk appeared indeed to display a slightly slower decay of expression [4]. However, the use of NIS may help to circumvent problems caused by immunogenicity of transgene products because it allows to use a species-specific isoform such as hNIS for humans. Efflux of ^{99m}Tc from the hNIS-expressing hearts was found in the present study as in the previous tumor studies [24,26]. Coupled with its short physical half-life (6 hrs), ^{99m}Tc may be applicable for repetitive and daily monitoring of vector activity both in the heart and in the whole body.

Future efforts may focus on substituting a cardiac tissue-specific promoter (e.g., Myosin light chain) for the constitutive CMV promoter to diminish extracardiac activity in other organs including the thyroid and the stomach, and to drive NIS expression preferably in the heart [31,32]. Additionally, adenovirus has been shown to elicit a strong host immune response, which hampers longitudinal imaging of reporter gene expression. Transient expression due to the immunogenic reaction is a well-known limitation of adenoviral vectors. Adenovirus was nevertheless chosen as vector in this study to obtain proof of principle for the usefulness of the hNIS gene as reporter gene because of long-term experience, easy production, and high transduction efficiency. This study provides the basis for a future use of hNIS with other vector types, because the basic principle of using a reporter gene for imaging is independent

of the vector used for transfer of the gene. Thus, the reporter system can be applied to, e.g., retrovirus or lentivirus, which are nonimmunogenic and produce stable transgene expression. Such vectors will be necessary for adequately monitoring the time course of transplanted cells after prior ex vivo transduction. Furthermore, the use of pinhole collimators will improve spatial resolution and detection sensitivity for small animal imaging; and single-photon emission tomography (SPECT) techniques can provide tomographic images using either ^{123}I or ^{99m}Tc [33]. Moreover, with use of ^{124}I , hNIS reporter system may also be applicable to clinical PET and microPET [3,29].

5. Conclusion

The hNIS gene is feasible for specific in vivo monitoring of magnitude and time course of cardiac transgene expression. Radioiodine and ^{99m}Tc are both suitable reporter probes, allowing for application of conventional gamma-camera imaging. This approach will increase availability of reporter gene imaging and facilitate development and monitoring of experimental and clinical cardiac molecular therapy in the future.

Acknowledgements

This study was supported by the Deutsche Forschungsgemeinschaft (Be 2217/4-1). The authors are grateful to John C. Morris, MD, Department of Endocrinology, Mayo Clinic, Rochester, MN, USA, for supplying the adenovirus expressing hNIS. The authors thank Bryan Essien for excellent technical assistance. We also thank the technologists of RI unit and animal care unit of the TU München for assistance in conduction of experiments, and we are indebted to Mrs. Raimonde Busch, Institute for Medical Statistics and Epidemiology, TU München, for statistical consultation.

References

- [1] Isner JM. Myocardial gene therapy. *Nature* 2002;415:234–9.
- [2] Forrester JS, Price MJ, Makkar RR. Stem cell repair of infarcted myocardium: an overview for clinicians. *Circulation* 2003;108:1139–45.
- [3] Wu JC, Inubushi M, Sundaresan G, Schelbert HR, Gambhir SS. Positron emission tomography imaging of cardiac reporter gene expression in living rats. *Circulation* 2002;106:180–3.
- [4] Inubushi M, Wu JC, Gambhir SS, Sundaresan G, Satyamurthy N, Namavari M, et al. Positron-emission tomography reporter gene expression imaging in rat myocardium. *Circulation* 2003;107:326–32.
- [5] Wu JC, Chen IY, Sundaresan G, Min J-J, De A, Qiao J-H, et al. Molecular imaging of cardiac cell transplantation in living animals using optical bioluminescence and positron emission tomography. *Circulation* 2003;108:1302–5.

- [6] Bengel FM, Anton M, Richter T, Simoes MV, Haubner R, Henke J, et al. Noninvasive imaging of transgene expression by use of positron emission tomography in a pig model of myocardial gene transfer. *Circulation* 2003;108:2127–33.
- [7] Carrasco N. Iodide transport in the thyroid gland. *Biochim Biophys Acta* 1993;1154:65–82.
- [8] Dai G, Levy O, Carrasco N. Cloning and characterization of the thyroid iodide transporter. *Nature* 1996;379:458–60.
- [9] Smanik PA, Liu Q, Furminger TL, Ryu K, Xing S, Mazzaferri EL, et al. Cloning of the human sodium iodide symporter. *Biochem Biophys Res Commun* 1996;226:339–45.
- [10] Spitzweg C, Dietz AB, O'Connor MK, Bergert ER, Tindall DJ, Young CYF, et al. In vivo sodium iodide symporter gene therapy of prostate cancer. *Gene Ther* 2001;8:1524–31.
- [11] Bengel FM, Anton M, Avril N, Brill T, Nguyen N, Haubner R, et al. Uptake of radiolabeled 2'-fluoro-2'-deoxy-5-iodo-1-β-D-arabinofuranosyluracil in cardiac cells after adenoviral transfer of the herpesvirus thymidine kinase gene the cellular basis for cardiac gene imaging. *Circulation* 2000;102:948–50.
- [12] Hitt M, Bett AJ, Addison CL, Prevec L, Graham FL. Techniques for human adenovirus vector construction and characterization. In: Adolph KW, editor. *Viral Gene Techniques*. San Diego: Academic Press; 1995. p. 13–30.
- [13] Weig HJ, Laugwitz KL, Moretti A, Kronsbein K, Städele C, Brüning S, et al. Enhanced cardiac contractility after gene transfer of V2 vasopressin receptors in vivo by ultrasound-guided injection or transcatheter delivery. *Circulation* 2000;101:1578–85.
- [14] Jacobs A, Tjuvajev JG, Dubrovin M, Akhurst T, Balatoni J, Beattie B, et al. Positron emission tomography-based imaging of transgene expression mediated by replication-conditional, oncolytic herpes simplex virus type 1 mutant vectors in vivo. *Cancer Res* 2001;61:2983–95.
- [15] Sambrook J, Fritsch E, Maniatis T. *Molecular Cloning. A Laboratory Manual*. New York: Cold Spring Harbour Laboratory Press; 1989. p. 7–52.
- [16] Filetti S, Bidart J-M, Arturi F, Caillou B, Russo D, Schlumberger M. Sodium/iodide symporter: a key transport system in thyroid cancer cell metabolism. *Eur J Endocrinol* 1999;141:443–57.
- [17] Shen DHY, Kloos RT, Mazzaferri EL, Jhiang SM. Sodium iodide symporter in health and disease. *Thyroid* 2001;11:415–25.
- [18] Kotzerke J, Fenchel S, Guhlmann A, Stabin M, Rentschler M, Knapp Jr FF, et al. Pharmacokinetics of ^{99m}Tc-pertechnetate and ¹⁸⁸Re-perrhenate after oral administration of perchlorate: option for subsequent care after the use of liquid ¹⁸⁸Re in a balloon catheter. *Nucl Med Commun* 1998;19:795–801.
- [19] Eskandari S, Loo DDF, Dai G, Levy O, Wright EM, Carrasco N. Thyroid Na⁺/I⁻symporter. Mechanism, stoichiometry, and specificity. *J Biol Chem* 1997;272:27230–8.
- [20] Riedel C, Dohan O, De la Vieja A, Ginter CS, Carrasco N. Journey of the iodide transporter NIS: from its molecular identification to its clinical role in cancer. *Trends Biochem Sci* 2001;26:490–6.
- [21] Cho J-Y. A transporter gene (sodium iodide symporter) for dual purposes in gene therapy: imaging and therapy. *Curr Gene Ther* 2002;2:393–402.
- [22] Chung J-K. Sodium iodide symporter: its role in nuclear medicine. *J Nucl Med* 2002;43:1188–200.
- [23] Spitzweg C, Zhang S, Bergert ER, Castro MR, McIver B, Heufelder AE, et al. Prostate-specific antigen (PSA) promoter-driven androgen-inducible expression of sodium iodide symporter in prostate cancer cell lines. *Cancer Res* 1999;59:2136–41.
- [24] Mandell RB, Mandell LZ, Link Jr CJ. Radioisotope concentrator gene therapy using the sodium/iodide symporter gene. *Cancer Res* 1999;59:661–8.
- [25] Boland A, Ricard M, Opolon P, Bidart J-M, Yeh P, Filetti S, et al. Adenovirus-mediated transfer of the thyroid sodium/iodide symporter gene into tumors for a targeted radiotherapy. *Cancer Res* 2000;60:3484–92.
- [26] Haberkorn U, Henze M, Altmann A, Jiang S, Morr I, Mahmut M, et al. Transfer of the human *NaI* symporter gene enhances iodide uptake in hepatoma cells. *J Nucl Med* 2001;42:317–25.
- [27] La Perle KMD, Shen D, Buckwalter TLF, Williams B, Haynam A, Hinkle G, et al. In vivo expression and function of the sodium iodide symporter following gene transfer in the MATLyLu rat model of metastatic prostate cancer. *Prostate* 2002;50:170–8.
- [28] Niu G, Gaut AW, Boles Ponto LL, Hichwa RD, Madsen MT, Graham MM, et al. Multimodality noninvasive imaging of gene transfer using the human sodium iodide symporter. *J Nucl Med* 2004;45:445–9.
- [29] Groot-Wassink T, Aboagye EO, Glaser M, Lemoine NR, Vassaux G. Adenovirus biodistribution and noninvasive imaging of gene expression in vivo by positron emission tomography using human sodium/iodide symporter as reporter gene. *Hum Gene Ther* 2002;13:1723–35.
- [30] M Anton, C Wittermann, R Haubner, MV Simoes, R Reder, B Essien, et al. Coexpression of herpesviral thymidine kinase reporter gene and VEGF gene for noninvasive monitoring of therapeutic gene transfer; in vitro- and initial in vivo-evaluation. *J. Nucl. Med.* 2004;45:1743–6.
- [31] Avril N, Bengel FM. Defining the success of cardiac gene therapy: how can nuclear imaging contribute? *Eur J Nucl Med Mol Imaging* 2003;30:757–71.
- [32] Franz WM, Rothmann T, Frey N, Katus HA. Analysis of tissue-specific gene delivery by recombinant adenoviruses containing cardiac-specific promoters. *Cardiovasc Res* 1997;35:560–6.
- [33] Strand SE, Ivanovic M, Erlandsson K, Franceschi D, Button T, Sjogren M, et al. Small animal imaging with pinhole single-photon emission tomography. *Cancer* 1994;73:981–4.